Intelligent Health Indicators Based on Semi-supervised Learning Utilizing Acoustic Emission Data

Moradi, Morteza; Broer, Agnes; Chiachío, Juan; Benedictus, Rinze; Zarouchas, Dimitrios

DOI
10.1007/978-3-031-07322-9_43

Publication date
2023

Document Version
Final published version

Published in
European Workshop on Structural Health Monitoring, EWSHM 2022, Volume 3

Intelligent Health Indicators Based on Semi-supervised Learning Utilizing Acoustic Emission Data

Morteza Moradi[1,2(✉)], Agnes Broer[1,2], Juan Chiachío[3], Rinze Benedictus[1], and Dimitrios Zarouchas[1,2]

[1] Structural Integrity and Composites Group, Aerospace Engineering Faculty, Delft University of Technology, Kluyverweg 1, 2629 HS Delft, P.O. Box 5058, 2600 GB Delft, The Netherlands
M.Moradi-1@tudelft.nl

[2] Center of Excellence in Artificial Intelligence for Structures, Prognostics and Health Management, Aerospace Engineering Faculty, Delft University of Technology, Delft, The Netherlands

[3] Department Structural Mechanics and Hydraulics Engineering, Andalusian Research Institute in Data Science and Computational Intelligence (DaSCI), University of Granada, 18001 Granada, Spain

Abstract. Health indicators are indices that act as intermediary links between raw SHM data and prognostic models. An efficient HI should satisfy prognostic requirements such as monotonicity, trendability, and prognosability in such a way that it can be effectively used as an input in a prognostic model for remaining useful life estimation. However, discovering or designing a suitable HI for composite structures is a challenging task due to the inherent complexity of the evolution of damage events in such materials. Previous research has shown that data-driven models are efficient for accomplishing this goal. Large labeled datasets, however, are normally required, and the SHM data can only be labeled, respecting prognostic requirements, after a series of nominally identical structures are tested to failure. In this paper, a semi-supervised learning approach based on implicitly imposing prognostic criteria is adopted to design a novel HI suitable. To this end, single-stiffener composite panels were subjected to compression-compression fatigue loading and monitored using acoustic emission (AE). The AE data after signal processing and feature extraction were fused using a multi-layer LSTM neural network with criteria-based hypothetical targets to generate an intelligent HI. The results confirm the performance of the proposed scenario according to the prognostic criteria.

Keywords: Prognostic and health management · Structural health monitoring · Intelligent health indicator · Semi-supervised deep neural network · Composite structures

1 Introduction

Composite structures have an essential role in a variety of industries, notably aerospace and wind energy because they are high-performance structures with high strength-to-weight and stiffness-to-weight ratios. They are, however, vulnerable to a variety of

P. Rizzo and A. Milazzo (Eds.): EWSHM 2022, LNCE 270, pp. 419–428, 2023.
https://doi.org/10.1007/978-3-031-07322-9_43

damage modes that could lead to unexpected failures during operation [1]. The damage process comprises a complex and partially unknown sequence of fracture events that creates a high level of uncertainty in the structural assessment.

The process of establishing a damage identification method for aerospace, civil, and mechanical engineering infrastructure is termed Structural Health Monitoring (SHM) [2], in which permanently installed sensors record data in order to be analyzed. A natural evolution of SHM is prognostic and health management (PHM), in which forecasts of remaining useful life (RUL) are updated on a regular basis utilizing sensor information. To be capable of predicting RUL, a health indicator (HI) appropriate for consideration in a prognostic algorithm [3] is required. HI is a distinguishing feature derived from SHM data that reflects the health condition of the structure being monitored.

Well-known metrics such as Monotonicity (Mo), Trendability (Tr), and Prognosability (Pr) can be used to test the suitability of HI [4, 5]. Mo evaluates the general rising or declining pattern of a variable during history, whereas Tr reflects the resemblance of variable trajectories. Pr is used to determine the distribution of a variable's ultimate value. The most common procedure for extracting an HI is to choose the best features as an HI or the principal constituent components of the HI based on these prognostic criteria. In this framework, some features will be ignored even though they do not fit the criteria, yet their fusion may meet the necessary criteria. To address this problem, the prognostic metrics could act as a supervisory function in the HI design process instead of simply being a way of measuring HI's efficiency. The Artificial Neural Network (ANN) is a helpful approach in the case of PHM [6, 7] and is a powerful mathematical method for entering this challenge. Notwithstanding, explicitly implementing the prognostic metrics (Mo, Tr, and Pr) into an ANN is difficult because the backpropagation algorithm involves the metrics' derivatives, which are difficult to calculate. Moreover, since the values of HIs are unavailable to be used as targets for ANN, a supervised learning algorithm cannot address this problem. As a result, the lack of a strategy to overcome this issue is evident.

Semi-supervised learning (SSL) has been proposed as a viable approach for prognostics with a linear degradation trend in the literature. However, no study has been conducted on the HI design by combining features using an SSL framework to fulfill the prognostic requirements. Because only prognostic metrics and end-of-life (EOL) are accessible to help the framework, the present study proposes an inductive SSL named "intrinsically semi-supervised" [8], which is an extended form of supervised learning to incorporate unlabeled observations into the objective function.

In the present work, twelve single-stiffener composite panels were monitored using the acoustic emission (AE) method during compression-compression (C-C) fatigue loading to evaluate the suggested approach. The main data set comprises six AE variables, which are referred to as "signal" henceforth: amplitude, rise time, duration, energy, counts, and RMS. The feature extraction (FE) procedure was conducted in the time and frequency domains, and the derived features were used as inputs to a semi-supervised deep neural network (SSDNN). To optimize network hyperparameters while taking holdout validation into account, a Bayesian optimizer was implemented.

2 Experimental Setup

C-C fatigue loadings were applied to twelve composite specimens (CSs), which are composed of a skin panel and a single T-shape stiffener based on an Embraer design. The skin and stiffener are manufactured of IM7/8552 carbon fiber-reinforced epoxy unidirectional prepreg with $[45/-45/0/45/90/-45/0]_S$ and $[45/-45/45/-45]_S$ layouts, correspondingly [9]. Figure 1 depicts the arrangement of the AE sensors as well as the panel size. An impact loading with 10 J energy was applied to all panels, which did not occur in the same locations but always in the stiffener area [10]. Five CSs 1, 2, 3, 7, and 8 were impacted from the start, and the rest after 5000 cycles. Three CSs 4, 5, and 6 also had disbond defects with dimensions of 15 × 20, 20 × 20, and 20 × 25 between the skin panel and the stiffener, which were introduced during fabrication.

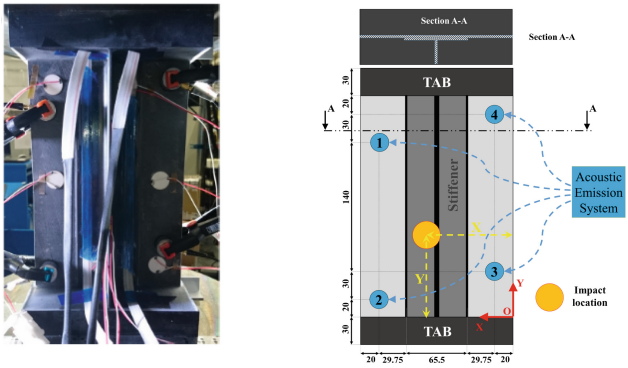

Fig. 1. (a) Stiffener side and (b) sensor coordinates (dimensions in [mm]) shown as blue circles. Locations of impact shown as a movable orange circle.

The CSs were loaded using an MTS machine at a frequency of 2 Hz and an R-ratio of 10, where a compression load was set in the range of [6.5, 65.0] kN. The fatigue loads were applied until the panels lost their load-bearing capability. Since AE data is included in the ReMAP project [10] and other SHM methods were used, the fatigue load was interrupted at 500-cycle intervals to allow the other SHM equipment to collect measurements.

Vallen Systeme GmbH VS900-M broadband sensors with a frequency band of 100–900 kHz were utilized as AE sensors. An AMSY-6 Vallen acquisition system was used to capture the AE hits. Vallen preamplifiers with a gain of 34 dB were also employed. Four AE sensors were attached to different locations on the skin of the CSs to form a parallelogram in order to localize damage. As shown in Fig. 1b, the [x, y] positions of the AE Sensors 1, 2, 3, and 4 were [145, 190], [145, 20], [20, 50], and [20, 220] mm, respectively.

To prevent recording background signals, an amplitude threshold of 60 dB was applied for detecting events. Only events occurring inside the AE sensor region are considered. For localization, the internal Vallen processor for planar positioning, which

is in accordance with Geiger's model, was employed [9, 11]. A filter was also applied to eliminate incidents with a location uncertainty of more than 50 mm. Six variables were selected and logged from AE events: amplitude (A), rise time (R), energy (E), counts (CNTS), duration (D), and RMS.

3 Workflow

This section describes the overall workflow, which comprises signal pre-processing, feature extraction (FE), and feature fusion (FF) with the product of HI.

3.1 Signal Pre-processing

Labeling cycles, time windowing, and missing values are all discussed in this subsection.

Labeling Cycles. Because HI will be constructed using a semi-supervised framework with consideration of hypothetical HIs as targets, the process of labeling cycles on AE data is essential for this framework. The cycle number of each hit could be approximated by signal processing methods using the captured displacement and load from the MTS machine.

Time Windowing. Signals such as amplitude, rising time, duration, energy, counts, and RMS are windowed for more efficient analysis. Because of the natural period of QS loads, the windowing process for the present research was conducted with a static length and interval of 500 cycles.

Missing Values. Due to the imposed filters, no events may have been logged in a few periods of 500 cycles, resulting in missing values for such time windows. Missing values should be removed or filled in since they affect succeeding steps of the HI building framework, with the first approach being used in the current study.

A zero-mean normalization, based on only the mean value and standard deviation from the training dataset, will be used after FE as another pre-processing action.

3.2 Feature Extraction (FE)

To begin, the Fast Fourier Transform (FFT) is used to map data from the time domain into the frequency domain as a standard and reasonable step toward improving FE. Following that, the common statistical features [12–14] from the time domain and frequency domain (Table 1) were extracted. According to Table 1, 33 features are obtained from each of the 6 windowed signals (amplitude, rise-time, energy, counts, duration, and RMS) of the AE dataset. The set of features has been expanded to include three new potentially helpful features: cumulative rise-time/amplitude ratio, cumulative energy, and cumulative counts [15]. As a result, the AE database provided 201 features ($6 \times 33 + 3$). It should be emphasized that the FE step can also be considered as a dimension reduction step, because raw signals with thousands or even millions of data points within each time window were compressed to 201 sample points.

Table 1. Statistical features in time and frequency domain.

No	Time domain features	No	Frequency domain features
1	$X_m = \frac{\sum_{n=1}^{N} x(n)}{N}$	20	$p_1 = X_{mf} = \frac{\sum_{k=1}^{K} s(k)}{K}$
2	$X_{sd} = \sqrt{\frac{\sum_{n=1}^{N} (x(n)-X_m)^2}{N-1}}$	21	$p_2 = \frac{\sum_{k=1}^{K} (s(k)-p_1)^2}{K-1}$
3	$X_{root} = \left(\frac{\sum_{n=1}^{N} \sqrt{\lvert x(n)\rvert}}{N}\right)^2$	22	$p_3 = \frac{\sum_{k=1}^{K} (s(k)-p_1)^3}{K\left(\sqrt{p_2}\right)^3}$
4	$X_{rms} = \sqrt{\frac{\sum_{n=1}^{N} (x(n))^2}{N}}$	23	$p_4 = \frac{\sum_{k=1}^{K} (s(k)-p_1)^4}{K{p_2}^2}$
5	$X_{rss} = \sqrt{\sum_{n=1}^{N} \lvert x(n)\rvert^2}$	24	$p_5 = X_{fc} = \frac{\sum_{k=1}^{K} f_k s(k)}{\sum_{k=1}^{K} s(k)}$
6	$X_{peak} = max\lvert x(n)\rvert$	25	$p_6 = \sqrt{\frac{\sum_{k=1}^{K} (f_k-p_5)^2 s(k)}{K}}$
7	$X_{skewness} = \frac{\sum_{n=1}^{N} (x(n)-X_m)^3}{(N-1){X_{sd}}^3}$	26	$p_7 = X_{rmsf} = \sqrt{\frac{\sum_{k=1}^{K} {f_k}^2 s(k)}{\sum_{k=1}^{K} s(k)}}$
8	$X_{kurtosis} = \frac{\sum_{n=1}^{N} (x(n)-X_m)^4}{(N-1){X_{sd}}^4}$	27	$p_8 = \sqrt{\frac{\sum_{k=1}^{K} {f_k}^4 s(k)}{\sum_{k=1}^{K} {f_k}^2 s(k)}}$
9	$X_{crest} = \frac{X_{peak}}{X_{rms}}$	28	$p_9 = \frac{\sum_{k=1}^{K} {f_k}^2 s(k)}{\sqrt{\sum_{k=1}^{K} s(k) \sum_{k=1}^{K} {f_k}^4 s(k)}}$
10	$X_{clearance} = \frac{X_{peak}}{X_{root}}$	29	$p_{10} = \frac{p_6}{p_5}$
11	$X_{shape} = \frac{X_{rms}}{\frac{1}{N}\sum_{n=1}^{N} \lvert x(n)\rvert}$	30	$p_{11} = \frac{\sum_{k=1}^{K} (f_k-p_5)^3 s(k)}{K{p_6}^3}$
12	$X_{impulse} = \frac{X_{peak}}{\frac{1}{N}\sum_{n=1}^{N} \lvert x(n)\rvert}$	31	$p_{12} = \frac{\sum_{k=1}^{K} (f_k-p_5)^4 s(k)}{K{p_6}^4}$
13	$X_{p2p} = \max(x(n)) - \min(x(n))$	32	$p_{13} = \frac{\sum_{k=1}^{K} \sqrt{(f_k-p_5)} s(k)}{K\sqrt{p_6}}$
14, 15, 16, 17	$X_{k\_cm} = \frac{\sum_{n=1}^{N} (x(n)-X_m)^k}{N}$; k = 3, 4, 5, 6	33	$p_{14} = \sqrt{\frac{\sum_{k=1}^{K} (f_k-p_5)^2 s(k)}{\sum_{k=1}^{K} s(k)}}$
18	$X_{FM4} = \frac{X_{4\_cm}}{{X_{sd}}^4}$		
19	$X_{med} = \frac{\sum_{n=1}^{N} t(n)}{N}$		

3.3 Feature Fusion

In this step, the extracted features are combined. This step's output is known as a "health indicator" (HI), and it will be used in a prognostic framework to forecast RUL. A HI should satisfy a number of metrics in order to be regarded as a prognostic parameter. Monotonicity (Mo), Prognosability (Pr), and Trendability (Tr) [4], which are employed in the current work, are three popular criteria for evaluating an HI and are formulated as follows:

$$\mathrm{Mo} = \mathrm{MMK} = \frac{1}{\mathrm{M}} \sum\nolimits_{\mathrm{j}=1}^{\mathrm{M}} \left| \frac{\sum_{\mathrm{i}=1}^{\mathrm{N_j}} \sum_{\mathrm{k}=1,\mathrm{k}>\mathrm{i}}^{\mathrm{N_j}} (\mathrm{t_k} - \mathrm{t_i}).\mathrm{sgn}(\mathrm{x}(\mathrm{t_k}) - \mathrm{x}(\mathrm{t_i}))}{(\mathrm{N_j} - 1) \sum_{\mathrm{i}=1}^{\mathrm{N_j}} \sum_{\mathrm{k}=1,\mathrm{k}>\mathrm{i}}^{\mathrm{N_j}} (\mathrm{t_k} - \mathrm{t_i})} \right| .100 \quad (1)$$

$$sgn(x) = \begin{cases} -1 \; if \; x < 0 \\ 0 \; if \; x = 0 \\ 1 \; if \; x > 0 \end{cases} \quad (2)$$

$$\mathrm{Tr} = \min_{\mathrm{j,k}} \left| \rho\left(\mathrm{x_j}, \mathrm{x_k}\right) \right|, \mathrm{j}, \mathrm{k} = 1, 2, \ldots, \mathrm{M} \quad (3)$$

$$\rho\left(\mathrm{x_j}, \mathrm{x_k}\right) = \frac{\mathrm{cov}\left(\mathrm{x_j}, \mathrm{x_k}\right)}{\sigma_{\mathrm{x_j}} \sigma_{\mathrm{x_k}}} \quad (4)$$

$$\mathrm{Pr} = \exp\left(- \frac{\left(\mathrm{std_j x_j}\left(\mathrm{N_j}\right)\right)}{\mathrm{mean_j}\left(\left|\mathrm{x_j}(1) - \mathrm{x_j}\left(\mathrm{N_j}\right)\right|\right)} \right), \; \mathrm{j} = 1, 2, \ldots, \mathrm{M} \quad (5)$$

where x_j denotes the vector of feature measurements on the j^{th} sample, M the number of samples monitored, and Nj the number of measurements on the j^{th} sample. t_k and t_i are the measurement times for $x(t_k)$ and $x(t_i)$, respectively. cov denotes the covariance, in which the standard deviations of x_j and x_k have been indicated by $\sigma(x_j)$ and $\sigma(x_k)$, respectively. To take into account all of the above prognostic metrics at the same time, an objective function named "Fitness" [5] is utilized:

$$\mathrm{Fitness} = \mathrm{a} \times \mathrm{Monotonicity_{HI}} + \mathrm{b} \times \mathrm{Prognosability_{HI}} + \mathrm{c} \times \mathrm{Trendability_{HI}} \quad (6)$$

where a, b, and c represent control factors that regulate the importance of each criterion in proportion to the rest. These factors are commonly user-defined parameters [5], which are typically expected to be in the [0–1] range. In this research, they are all regarded as one, yielding a fitness score of [0–3]. In current research, incorporating these metrics into the fusion step is one of the most essential and challenging phases.

Semi-supervised Criteria-Based Fusion Neural Network. The current work proposes a fusion model based on deep neural network (DNN) and semi-supervised learning (SSL). Inductive learning algorithms, termed intrinsically semi-supervised [8], are improvements to preexisting supervised algorithms that enable labelled and unlabeled data to be used directly to optimize an objective function with components.

In this research, a semi-supervised deep neural network (SSDNN) is proposed to generate HI using feature fusion through implicitly implementing the prognostic metrics as well as exploiting the given EOL. As can be seen in Fig. 2, following the prognostic criteria, a hypothesized optimal HI function is defined and then utilized as an objective for a supervised ANN to simulate the HI function.

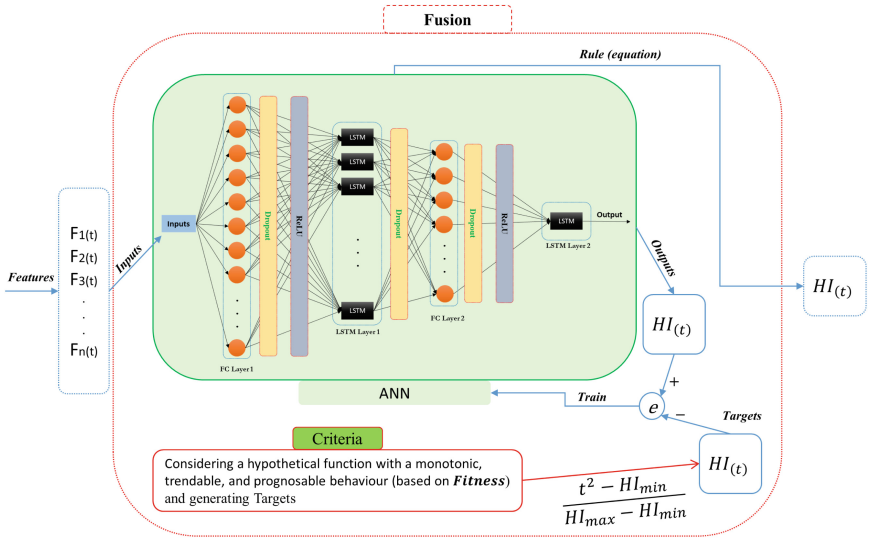

Fig. 2. The proposed semi-supervised criteria-based fusion neural network for HI construction.

To choose the optimum function, four primary functions with high compatibility with the metrics are investigated, which are linear ($HI_t = t$), quadratic polynomial ($HI_t = t^2$), natural logarithm ($HI_t = \ln(t)$), and exponential functions ($HI_t = \exp(t)$). Such functions should be characterized in terms of usage time, which is fatigue cycles in this work. To adapt Pr as a recursive reconstruction process of HI, the functions should be standardized by using max-min normalization.

Three synthetic specimens with different lifespans of 7, 4, and 10 time units (time step is 0.05) are adopted to evaluate the prognostic metrics. Based on the calculated criteria, all functions perfectly suit Mo and Pr, yet only linear and quadratic polynomial ones have the maximum value (1) of Tr. Because damage propagation and accumulation nonlinearity should be reflected in the HI trend, the quadratic polynomial function is employed to form the targets.

Because the database for the analyzed composite structures is new and no existing research has been done on them, simple shallow designs such as Multi-Layer Perceptrons (MLPs) were used to generate HI at first, prior to actually evolving into more complex networks. Each layer was inserted one by one, the number of hidden neurons at each layer was increased, and then the next layer was inserted. In the meantime, different kinds of layers, including the Fully Connected (FC) layer and Long Short-Term Memory (LSTM), were examined to produce more suitable results. The finalized DNN architecture is composed of the following layers: FC, Dropout, (Rectified Linear Units) ReLU, LSTM, and Regression layers.

Evaluation Metric and Hyperparameters Optimization. The Bayesian optimization algorithm was utilized to determine the optimal hyperparameters' sets, such as the number of hidden neurons in each layer, batch size, and dropout. To this end, according to the holdout validation method, 10, 1, and 1 CSs were regarded as training,

validation, and test datasets, respectively. For this optimization problem, the maximum RMSE over all CSs as the objective function must be minimized. It should be underlined that by evaluating the maximum RMSE of all CSs instead of other statistical characteristics such as their mean RMSE, the optimizer tries to simultaneously reduce the mean value and standard deviation of RMSE, which is more desired.

4 Results and Discussions

The deep learning model was trained using an Adam optimizer [16], with an initial learning rate of 0.005, a learning rate drop factor of 0.2, a learning rate drop period of 5, and a gradient threshold of 1, all of which were chosen through trial and error. The training dataset was shuffled before each epoch. Despite having a maximum of 500 training epochs, the network's output was exported according to the minimum validation loss, where the frequency of the validation check was adjusted to 30 trials (number of trained batches) and the validation check tolerance was adjusted to 6.

The number of neurons and units in the hidden layers based on trial and error as well as the batch size range based on the number of CSs in the training dataset, have been adjusted. Because each set of Bayesian optimization final outcomes is also conditional on the initial start points, the whole procedure was performed several times. Table 2 shows the five top hyperparameter sets. As can be seen, the configurations resulted in a very narrow RMSE range of [0.08–0.11], which is the maximum RMSE across all CSs as the objective function of the Bayesian optimizer.

Table 2. The top 5 hyperparameter sets (models) determined by the Bayesian optimization algorithm and holdout validation with 11th CS as the validation and the 12th CS as the test dataset. RMSE is the maximum one over all CSs. [initial: step size: end]

Model (rank)	Batch size [1: 1: 5]	Dropout [0: 0.1: 0.5]	FCL1 [1: 1: 201]	LSTM1 [1: 1: 256]	FCL2 [1: 1: 50]	*RMSE*
1	4	0.3	110	154	50	*0.0829*
2	5	0.4	124	83	48	*0.0884*
3	5	0.5	201	79	36	*0.0983*
4	5	0.4	152	81	27	*0.1013*
5	5	0.5	41	142	43	*0.1026*

Figure 3 depicts the constructed HIs by model 1, which is ranked first. Figure 4 shows the prognostic metrics for all individual input features alongside the HIs generated by model 1. The top four features with a fitness score greater than 1.5 are:

- feature 185 (1.630): the 6th-order central moment of the RMS signal in the time domain
- feature 184 (1.599): the 5th-order central moment of the RMS signal in the time domain
- feature 88 (1.586): the variance of the Energy signal in the frequency domain
- feature 183 (1.566): the 4th-order central moment of the RMS signal in the time domain

The high Fitness score of 2.891 for HIs, which is 77.3% greater than the best feature (1.630), shows model 1's outstanding efficiency in constructing HIs.

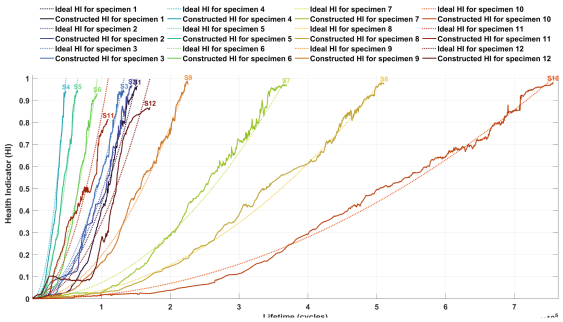

Fig. 3. HIs constructed by model 1. The validation and test datasets are CS 11 and 12, respectively, and the others are training datasets. Dot lines show ideal HIs.

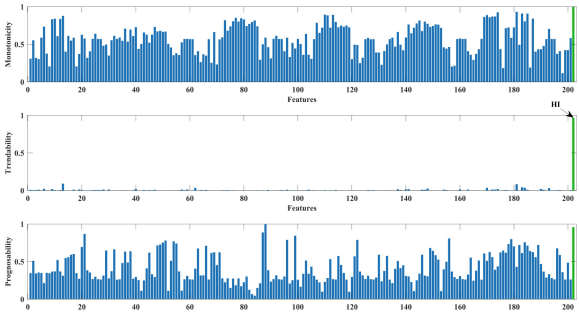

Fig. 4. The prognostic metrics for all 201 extracted features and the constructed HIs for model 1.

5 Conclusions

To address the shortage of labeled data, a semi-supervised deep neural network (SSDNN) was proposed to implicitly induce a multi-layer LSTM network that fulfills the prognostic requirements and was applied to a case study involving AE data collected during fatigue tests of composite specimens. A Bayesian optimizer used for holdout validation yielded five top models. The high Fitness score of 2.891 for HIs (maximum Fitness is 3) showed model 1's high performance in creating HIs based on prognostic metrics, which is 77.3% greater than the best input feature (1.6303) and demonstrates the efficiency of the suggested framework. For this improvement, the prognostic metrics were included within the feature fusion and HI construction framework instead of being employed merely as an HI quality measuring device.

Funding. This project has received funding from the European Union's Horizon 2020 research and innovation programme under the Marie Sklodowska-Curie grant agreement No 859957 "ENHAnCE, European training Network in intelligent prognostics and Health mAnagement in Composite structurEs" and grant agreement No 769288 "ReMAP, Real-time Condition-based Maintenance for Adaptive Aircraft Maintenance Planning".

References

1. Ameri, B., Moradi, M., Mohammadi, B., Salimi-Majd, D.: Investigation of nonlinear post-buckling delamination in curved laminated composite panels via cohesive zone model. Thin-Walled Struct. **154**, 106797 (2020)
2. Farrar, C.R., Worden, K.: An introduction to structural health monitoring. Philos. Trans. Roy. Soc. A: Math. Phys. Eng. Sci. **365**(1851), 303–315 (2007)
3. Galanopoulos, G., Milanoski, D., Broer, A., Zarouchas, D., Loutas, T.: Health monitoring of aerospace structures utilizing novel health indicators extracted from complex strain and acoustic emission data. Sensors **21**(17), 5701 (2021)
4. Coble, J., Hines, J.W.: Identifying optimal prognostic parameters from data: a genetic algorithms approach. In: Annual Conference of the PHM Society, vol. 1, no. 1 (2009)
5. Eleftheroglou, N.: Adaptive prognostics for remaining useful life of composite structures (2020)
6. Fink, O., Wang, Q., Svensen, M., Dersin, P., Lee, W.-J., Ducoffe, M.: Potential, challenges and future directions for deep learning in prognostics and health management applications. Eng. Appl. Artif. Intell. **92**, 103678 (2020)
7. Khan, S., Yairi, T.: A review on the application of deep learning in system health management. Mech. Syst. Signal Process. **107**, 241–265 (2018)
8. van Engelen, J.E., Hoos, H.H.: A survey on semi-supervised learning. Mach. Learn. **109**(2), 373–440 (2019). https://doi.org/10.1007/s10994-019-05855-6
9. Broer, A.A.R., Galanopoulos, G., Zarouchas, D., Loutas, T., Benedictus, R.: Damage diagnostics of a composite single-stiffener panel under fatigue loading utilizing SHM data fusion. In: Rizzo, P., Milazzo, A. (eds.) EWSHM 2020. LNCE, vol. 127, pp. 616–625. Springer, Cham (2021). https://doi.org/10.1007/978-3-030-64594-6_60
10. Zarouchas, D., Broer, A., Galanopoulos, G., Briand, W., Benedictus, R., Loutas, T.: Compression compression fatigue tests on single stiffener aerospace structures, V1 ed: DataverseNL (2021)
11. Broer, A., Galanopoulos, G., Benedictus, R., Loutas, T., Zarouchas, D.: Fusion-based damage diagnostics for stiffened composite panels. Structural Health Monitoring 14759217211007127 (2021)
12. Lei, Y.: Intelligent Fault Diagnosis and Remaining Useful Life Prediction of Rotating Machinery. Butterworth-Heinemann (2016)
13. Paulter, N.G., Larson, D.R., Blair, J.J.: The IEEE standard on transitions, pulses, and related waveforms, Std-181-2003. IEEE Trans. Instrument. Meas. **53**(4), 1209–1217 (2004)
14. Daponte, P.: IEEE standard on transitions, pulses, and related waveforms (2003)
15. Saeedifar, M., Zarouchas, D.: Damage characterization of laminated composites using acoustic emission: a review. Compos. B Eng. **195**, 108039 (2020)
16. Kingma, D.P., Ba, J.: Adam: a method for stochastic optimization. arXiv preprint arXiv: 1412.6980 (2014)